ФИЗИКА ЭЛЕМЕНТАРНЫХ ЧАСТИЦ И АТОМНОГО ЯДРА
2015. Т. 46. ВЫП. 5

NEUTRON STAR PROPERTIES FROM THE POSTMERGER GRAVITATIONAL WAVE SIGNAL OF BINARY NEUTRON STARS

A. Bauswein [1,*], *N. Stergioulas* [1], *H.-T. Janka* [2]

[1] Department of Physics, Aristotle University of Thessaloniki, Thessaloniki, Greece

[2] Max-Planck-Institut für Astrophysik, Garching, Germany

We discuss the equation-of-state dependence of the gravitational wave (GW) signal of neutron star mergers. For a given binary mass, the dominant oscillation frequency of the postmerger remnant scales tightly with neutron star radii of a given mass. This relation means that a measurement of the dominant GW frequency, when combined with information from the inspiral phase, implies a simultaneous mass and radius measurement. Moreover, we derive a procedure by which the detection of two merger events with somewhat different binary masses can be employed for an estimate of the maximum mass of nonrotating neutron stars, the radius of the maximum-mass configuration, and the maximum central density of neutron stars. Compared to our method recently described in [7], we here employ a slightly modified procedure.

PACS: 97.60.Jd

INTRODUCTION

High-density physics is tightly connected to the stellar structure of neutron stars (NSs), since the latter is fully determined by the equation of state (EoS) of high-density matter (in a given theory of gravity). This stresses the importance to measure NS properties, such as a point on the unique mass–radius relation, apart from laboratory experiments and theoretical approaches to study the conditions of high-density matter. A sufficiently strong phase transition may leave an imprint on the mass–radius relation, too. Finally, whether or not a phase transition occurs in compact stars depends on the highest possible density in such objects, which is presumably also the highest density which can stably exist in the Universe.

Here we report a method for how the stellar structure of NSs can be derived from gravitational wave (GW) detections of NS mergers (see, e.g., [1] for a review

*E-mail: bauswein@mpa-garching.mpg.de

on the underlying physics of such events, their numerical modelling, the historical evolution of the field and a more thorough collection of references). Such measurements may become possible with the next generation of GW detectors, which are going into operation within a few years. We focus on the postmerger phase of NS coalescences which typically result in the formation of a strongly oscillating, rotating massive merger remnant (e.g., [2–6]). We show that the observation of the dominant oscillation frequency of the postmerger remnant can be employed to infer the radius of an NS with a given mass, implying a simultaneous mass and radius measurement [2, 3]. Moreover, we present a procedure to derive the maximum mass of nonrotating NSs and the radius of the maximum-mass configuration [7]. The same approach allows one to derive the maximum density of NSs. Note that we use a slightly modified procedure compared to [7].

1. RADIUS MEASUREMENTS

We employ hydrodynamical simulations of NS mergers for a large sample of candidate EoSs which include temperature effects consistently. Details on the numerical modelling, the dynamics, and the resulting GW signal can be found in [3, 8, 9]. The dominant postmerger oscillation frequency is extracted from the GW spectrum, which exhibits a *pronounced peak* in the kHz range. This dominant oscillation of the merger remnant has been found to be the *quadrupolar fluid mode* [10]. It is important to stress that the GW inspiral signal determines the binary mass and mass ratio (as combinations of them are intrinsic parameters of the GW search algorithm). Therefore, one can focus on the results for a given binary system keeping in mind that similar results can be obtained for any other binary configuration that could potentially be detected. We consider the merger of two stars with $1.35M_{\odot}$, which represent the most common binary configuration according to pulsar observations.

Figure 1, *a* displays the dominant postmerger GW frequency $f_{\rm peak}$ for 1.35–$1.35M_{\odot}$ binaries for different EoSs. The EoS dependence is visualized by showing the frequency as a function of the radius $R_{1.6}$ of a nonrotating NS with $1.6M_{\odot}$. The radius $R_{1.6}$ is an unambiguous function of the EoS as solution of the Tolman–Oppenheimer–Volkoff (TOV) equations. The tight relation between $f_{\rm peak}$ and $R_{1.6}$ implies that a measurement of the dominant GW oscillation frequency determines accurately the radius of a $1.6M_{\odot}$ NS, being equivalent to a simultaneous mass and radius observation of an NS. The scatter from the relation is of the order of 100–200 m, which determines the error of a radius measurement by an observation of $f_{\rm peak}$. Recently, it has been shown that the peak frequency $f_{\rm peak}$ can be measured accurately in a GW observation for sufficiently close events [11]. In this work, model waveforms taken from our simulations have been superimposed with measured noise from a LIGO science run. The noise has been rescaled to the anticipated sensitivity of the next-generation detec-

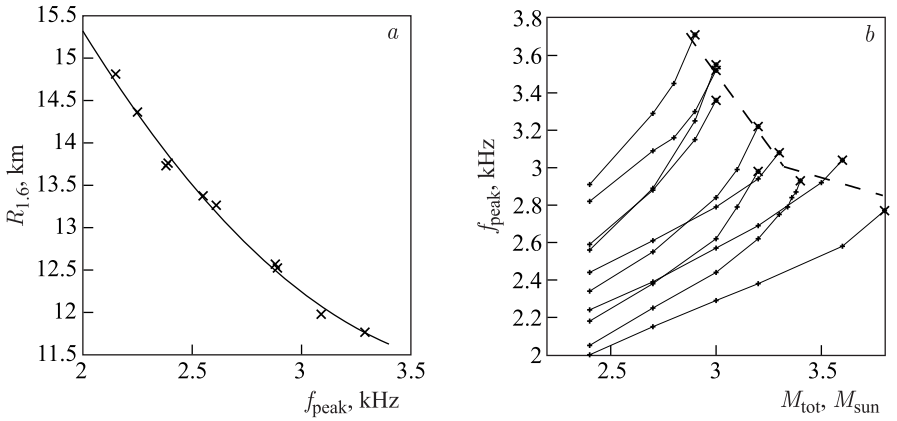

Fig. 1. *a*) Dominant GW oscillation frequency of the postmerger phase as a function of the radius $R_{1.6}$ of nonrotating NS with $1.6M_{\odot}$ for different EoSs. *b*) Dominant GW oscillation frequency of the postmerger phase as a function of the binary mass $M_{\rm tot}$ for different EoSs (solid lines). The crosses mark the threshold mass and the associated oscillation frequency. The threshold indicates the most massive binary mass for which a postmerger remnant forms instead of the direct collapse to a black hole after coalescence. (Figures taken from [7])

tors, and the peak frequencies $f_{\rm peak}$ of the injected model waveforms have been successfully recovered by existing GW data analysis pipelines.

The peak frequency also forms a relation with $R_{1.35}$, which is the radius of the inspiralling stars, implying that also the radius of a nonrotating NS with $1.35M_{1.35}$ can be obtained from a detection of the peak frequency of $1.35{-}1.35M_{\odot}$ binary. However, the scatter in the relation is somewhat larger compared to that in Fig. 1, *a*. This is a consequence of the increase of the density in the postmerger remnant, which thus probes the density regime of NSs more massive than the inspiralling ones and explains the tighter relation for $R_{1.6}$. Relations similar to the one shown in Fig. 1, *a* also exist for other binary masses including asymmetric systems. Note that also the GW inspiral signal preceding the merger may determine the radii of the inspiralling stars because finite-size effects influence the exact waveform in the last phase before merging (e.g., [12]).

2. ESTIMATING PROPERTIES OF THE MAXIMUM-MASS CONFIGURATION

For typical binary masses, an NS coalescence results in the formation of a postmerger remnant, and a characteristic peak frequency $f_{\rm peak}$ can be extracted. Only for relatively high binary masses, the coalescence leads to the direct formation of a black hole. The threshold binary mass for black hole formation depends

on the EoS and can be expressed by the maximum mass $M_{\rm max}$ of nonrotating NSs and the radius $R_{\rm max}$ of the maximum mass configuration [5].

Figure 1, *b* clarifies how the peak frequency depends on the total binary mass for different EoSs. The plus signs show the peak frequency extracted from simulations for different binary masses. The solid lines connect the results for a given EoS. For a given EoS, the peak frequency increases with mass which is understandable from the fact that the remnant becomes more compact and thus its oscillation frequency is higher. A sequence for a given EoS terminates at some characteristic threshold mass $M_{\rm thres}$, indicated by a cross in Fig. 1, *b*. For a given EoS, the cross marks the highest possible binary mass that leads to an NS postmerger remnant and the associated peak frequency, which we call $f_{\rm thres}$. It is apparent from Fig. 1, *b* that $M_{\rm thres}$ and $f_{\rm thres}$ are approximately correlated, which is indicated by the dashed line.

The continuous behavior of $f_{\rm peak}(M_{\rm tot})$ and the unique relation between $M_{\rm thres}$ and $f_{\rm thres}$ can be employed to estimate the threshold mass and threshold frequency. If GW measurements of two NS merger events reveal the peak frequency of *two different* binary masses $M_{\rm tot}$, one can extrapolate $f_{\rm peak}(M_{\rm tot})$ along the solid curve of the true EoS, e.g., by a linear extrapolation. The intersection of the extrapolating line estimates $M_{\rm thres}$ and $f_{\rm thres}$ of the true EoS. Importantly, this estimate can be obtained from detections of relatively low binary masses, e.g., in the range $M_{\rm tot} \sim 2.4{-}2.8 M_{\odot}$, which may be crucial because binaries with masses near $M_{\rm thres}$ are not expected to be very common. Note that the binary masses are given by the GW inspiral signal and that small asymmetries do not alter the peak frequency significantly.

While a simple linear extrapolation of $f_{\rm peak}(M_{\rm tot})$ already yields satisfactory estimates of $M_{\rm thres}$ and $f_{\rm thres}$, the procedure can be refined to accommodate the bending of the $f_{\rm peak}(M_{\rm tot})$ curve towards the threshold. The exact method has been described in detail in [7] and yields even more accurate estimates of $M_{\rm thres}$ and $f_{\rm thres}$ assuming only two measurements of $f_{\rm peak}$ at (somewhat) different $M_{\rm tot}$.

Recently, we found empirically that the threshold mass $M_{\rm thres}$ is a function of $M_{\rm max}$ and $R_{\rm max}$ (the mass and radius of the maximum-mass TOV star) [5]. Moreover, $f_{\rm thres}$ scales very well with $R_{\rm max}$. These empirical relations imply that an estimate of $M_{\rm thres}$ and $f_{\rm thres}$ can be used to infer $M_{\rm max}$ and $R_{\rm max}$: first $f_{\rm thres}$ provides $R_{\rm max}$, so that $M_{\rm thres}$ becomes a function of $M_{\rm max}$ only. This function is then inverted to obtain the maximum mass. The details of the extrapolation method and the inversion to obtain $R_{\rm max}$ from $M_{\rm thres}$ can be found in [7].

While following the same idea, we report here the results for a slightly modified procedure. By this we would like to emphasize the robustness of our procedure with respect to the details of the method. Moreover, in the future it may turn out that for a larger set of EoS models (or a more detailed modelling of the merger event) one or the other specifications of the procedure may yield more ac-

curate estimates. Compared to [7], we modify the procedure in two ways. In [7], we used the fact that $M_{\rm thres}$ can also be described as a function of $M_{\rm max}$ and $R_{1.6}$. Hence, we employed the peak frequency of a $1.35{-}1.35M_{\odot}$ binary merger to determine $R_{1.6}$ as in Sec. 1, and then obtained $M_{\rm max}$ from the $M_{\rm thres}$ estimate. As described above, we here use the direct $R_{\rm max}$ estimate from the extrapolation to $f_{\rm thres}$, which may be more useful if the dependence of $M_{\rm thres}$ on $M_{\rm max}$ and $R_{\rm max}$ turns out to be more robust for a larger sample of EoSs. Moreover, we use slightly different prescriptions of the extrapolation for $M_{\rm thres}$ on the one hand and $f_{\rm thres}$ on the other hand, which result in slightly better estimates for both quantities (the σ parameter of [7] is chosen to be 0.1 for the $f_{\rm thres}$ estimate while we use the same σ as in [7] for the $M_{\rm thres}$ determination). While this represents only a minor tuning, at this stage it is empirically justified, and it remains to be checked whether there are deeper reasons for the improvement. In any case, it shows that tuning the extrapolation procedure may yield better estimates.

Using the procedure sketched above, in Fig. 2 is shown the estimated $M_{\rm max}$ and $R_{\rm max}$ (circles) together with the real mass-radius relations (solid lines). In addition, we mark the real maximum-mass configuration by a cross, which should be compared with the circle of the same color corresponding to the same EoS. We stress once more that the estimate has been derived from the GW peak frequencies of two different merger events at somewhat different binary masses near $2.7M_{\rm tot}$, thus the most likely observations one can hope for with the upcoming GW instruments. Figure 2 illustrates that our procedure determines $M_{\rm max}$ and $R_{\rm max}$ very accurately from GW observations of the postmerger frequency. The maximum mass is revealed with an error better than $0.18M_{\odot}$ (this is the largest

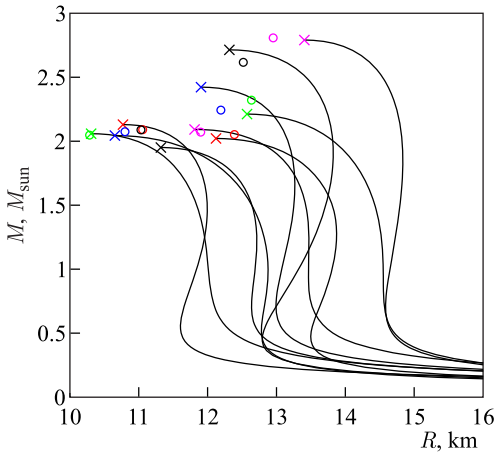

Fig. 2. Estimated stellar properties of the maximum-mass TOV configuration (circles) compared to the true values of $M_{\rm max}$ and $R_{\rm max}$ (crosses) together with the mass-radius relations (solid lines) for different EoSs

deviation between estimated and true $M_{\rm max}$ among our sample of EoSs). The deviations are actually significantly better than those for most EoSs. The radius $R_{\rm max}$ of the maximum-mass configuration is estimated with an error better than 450 m. Note that these estimates are slightly better than in [7] as a result of the modifications of the extrapolation procedure, demonstrating the possibility of refining the method for even better estimates.

We would like to mention that already a single, even rough GW measurement of $f_{\rm peak}$ for a given $M_{\rm tot}$ (derived from the inspiral signal) may be useful for a rough estimate of $M_{\rm max}$ and $R_{\rm max}$. Such a measurement would determine a single point on the $f_{\rm peak}(M_{\rm tot})$ curve of the true EoS. Making reasonable assumptions about the slope of the $f_{\rm peak}(M_{\rm tot})$ curve, which may be inspired by numerical data, one may determine a range of possible $M_{\rm thres}$ and $f_{\rm thres}$. This range may then be inverted to yield a range or constraint on $M_{\rm max}$ and $R_{\rm max}$. Of course, the accuracy of the constraint will depend on the exact binary system observed and on the EoS, i.e., how close the measured point is to the threshold.

Finally, we remark that $f_{\rm thres}$ has been found to scale also with the maximum rest-mass density $\rho_{\rm max}$ of nonrotating NSs (see Figs. 9 and 10 in [7]). This relation can be employed to determine $\rho_{\rm max}$ from GW detections in the same way as we described above, namely, by using the extrapolation procedure to obtain an estimate of $f_{\rm thres}$ and by inverting the empirical relation $f_{\rm thres}(\rho_{\rm max})$. Doing so, future GW observations may yield the maximum rest-mass density of NSs with an accuracy of only 10 per cent.

CONCLUSIONS

In this proceedings contribution, we report on how GW observations of NS mergers determine stellar properties of NSs. By detecting the dominant oscillation frequency of the postmerger remnant, one can obtain accurate simultaneous mass and radius measurements. Moreover, two events with somewhat different binary masses can be employed to infer the maximum mass of nonrotating NSs, the radius of the maximum-mass configuration and the maximum central density of NSs.

Acknowledgements. A. B. is a Marie Curie Intra-European Fellow within the 7th European Community Framework Programme (IEF 331873). This work was supported by the Deutsche Forschungsgemeinschaft through Sonderforschungsbereich Transregio 7 “Gravitational Wave Astronomy”, and the Cluster of Excellence EXC 153 “Origin and Structure of the Universe”. Partial support comes from “NewCompStar”, COST Action MP1304. The authors acknowledge support through the INT program INT-14-2a “Binary Neutron Star Coalescence as a Fundamental Physics Laboratory”. The computations discussed here were performed at the Rechenzentrum Garching of the Max-Planck-Gesellschaft, the Max Planck Institute for Astrophysics, and the Cyprus Institute under the LinkSCEEM/CyTera project.

REFERENCES

1. *Faber J. A., Rasio F. A.* Binary Neutron Star Mergers // Living Rev. Rel. 2012. V. 15. P. 8.
2. *Bauswein A., Janka H.-T.* Measuring Neutron Star Properties via Gravitational Waves from Neutron Star Mergers // Phys. Rev. Lett. 2012. V. 108. P. 011101.
3. *Bauswein A. et al.* Equation-of-State Dependence of the Gravitational Wave Signal from the Ring-Down Phase of Neutron Star Mergers // Phys. Rev. D. 2012. V. 86. P. 063001.
4. *Hotokezaka K. et al.* Remnant Massive Neutron Stars of Binary Neutron Star Mergers: Evolution Process and Gravitational Waveform // Phys. Rev. D. 2013. V. 88. P. 044026.
5. *Bauswein A. et al.* Prompt Merger Collapse and the Maximum Mass of Neutron Stars // Phys. Rev. Lett. 2013. V. 111. P. 131101.
6. *Takami K. et al.* Constraining the Equation of State of Neutron Stars from Binary Mergers. arxiv:1403.5672. 2014.
7. *Bauswein A. et al.* Revealing the High-Density Equation of State Through Binary Neutron Star Mergers // Phys. Rev. D. 2014. V. 90. P. 023002.
8. *Oechslin R. et al.* Relativistic Neutron Star Merger Simulations with Nonzero Temperature Equations of State. I. Variation of Binary Parameters and Equation of State // Astron. Astrophys. 2007. V. 467. P. 395.
9. *Bauswein A. et al.* Testing Approximations of Thermal Effects in Neutron Star Merger Simulations // Phys. Rev. D. 2010. V. 82. P. 084043.
10. *Stergioulas N. et al.* Gravitational Waves and Nonaxisymmetric Oscillation Modes in Mergers of Compact Object Binaries // Mon. Not. Roy. Astron. Soc. 2011. V. 418. P. 427.
11. *Clark J. et al.* Prospects for High Frequency Burst Searches Following Binary Neutron Star Coalescence with Advanced Gravitational Wave Detectors // Phys. Rev. D. 2014 (submitted).
12. *Read J. S. et al.* Matter Effects on Binary Neutron Star Waveforms // Phys. Rev. D. 2013. V. 88. P. 044042.